

Effect of process parameters on tensile strength of friction stir welded cast A356 aluminium alloy joints

M. JAYARAMAN¹, V. BALASUBRAMANIAN²

1. Paavaai Group of Institutions-Integrated Campus, School of Engineering, NH-7,
Paavaai Vidhya Nagar, R. Puliampatti, Puduchatram (Post) Namakkal – 637 018, Tamil Nadu, India;
2. Centre for Materials Joining & Research (CEMAJOR), Department of Manufacturing Engineering,
Annamalai University, Annamalai Nagar – 608 002, Tamil Nadu, India

Received 2 February 2012; accepted 24 May 2012

Abstract: A356 is a high strength aluminium–silicon cast alloy used in food, chemical, marine, electrical and automotive industries. Fusion welding of this cast alloy will lead to many problems such as porosity, micro-fissuring, and hot cracking. However, friction stir welding (FSW) can be used to weld this cast alloy without above mentioned defects. An attempt was made to study the effect of FSW process parameters on the tensile strength of cast A356 aluminium alloy. Joints were made using different combinations of tool rotation speed, welding speed and axial force. The quality of weld zone was analyzed by macrostructure and microstructure analyses. Tensile strengths of the joints were evaluated and correlated with the weld zone hardness and microstructure. The joint fabricated using a rotational speed of 1000 r/min, a welding speed of 75 mm/min and an axial force of 5 kN showed a higher tensile strength compared to the other joints.

Key words: A356 aluminium alloy; friction stir welding; tool rotation speed; welding speed; axial force; tensile strength

1 Introduction

Fusion welding of cast aluminium alloys is generally difficult due to some common defects occurring in the welds such as porosity, oxide inclusion, hot cracking which in turn reduce the joint strength [1]. In recent years, friction stir welding (FSW) has been found to be very effective for the welding of various wrought aluminum alloys. Friction stir processing (FSP) technique has been developed based on FSW for improving the mechanical properties of cast A356 aluminium alloy by eliminating the porosity. Also the microstructure gets refined due to the stirring action [2]. Moreover, the super plasticity and fatigue properties are improved considerably [3].

Dissimilar plate welding was made with Al 6061-T651 rolled plate and A356-T6 cast plate by FSW. The elongation of the joint was found to be lower than that of the uni-alloy joint [4]. The mechanical properties of cast A319 Al alloy was improved by FSP because of reduction in the size of second phase particles, uniform

distribution of Si particles and reduction in percentage of porosity volume [5]. The tensile strength and hardness of ADC12 aluminum die cast alloy were improved by FSP which was attributed to the elimination of cold flake, uniform dispersion of Si particles and the grain refinement of aluminium matrix [6]. Tool rotation rate and traverse speed showed significant influence on the microstructure and macrostructure of the friction stir processed cast A356 Al alloy [7]. The strength and ductility of the multi pass FSP nugget zone in A356 were similar to those achieved in the single-pass FSP treated sample [8].

Empirical relationships were developed between the mechanical properties of different grades of wrought aluminum alloys and FSW process parameters [9]. It is already known that the joint between cast Al alloys has a potential for expanding the usage of economic casting in airframe and missile applications. However, the investigations on FSW of cast aluminium alloys are very limited. To widen applications of FSW process to cast aluminium alloys, it is necessary to study joint properties of the cast alloys. Hence, an attempt was made to

understand the effect of FSW process parameters on tensile strength of cast A356 (also known as LM25) aluminium alloy.

2 Experimental

Castings of unmodified A356 aluminium alloy were made by sand casting method and they were machined to rectangular plates of 175 mm×75 mm×6 mm. The chemical composition of A356 alloy is presented in Table 1. Square butt joint configuration, as shown Fig. 1, was prepared to fabricate FSW joints. The initial joint configuration was obtained by securing the plates in position using mechanical clamps. Non-consumable tool made of high carbon steel was used to fabricate the joints. Friction stir welding machine with a capacity of 11 kW, 3000 r/min and 25 kN was used to fabricate the joints. Joints were fabricated using different combinations of tool rotation speed, traverse speed and axial force. The levels of process parameters and tool dimensions are presented in Table 2.

Table 1 Chemical composition of A356 cast aluminium alloy (mass fraction, %)

Si	Mg	Fe	Cu	Mn	Zn	Ni	Al
6.87	0.49	0.28	0.1	0.05	0.09	0.01	Bal.

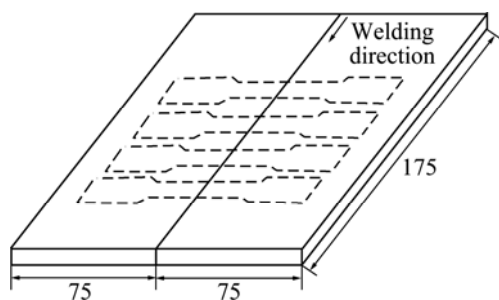


Fig. 1 Scheme of welding and extraction of tensile specimens (unit: mm)

Table 2 FSW process parameters and tool dimensions

Process parameter	Value
Tool rotation speed/(r·min ⁻¹)	900, 1000, 1200, 1400
Welding speed/(mm·min ⁻¹)	22, 40, 75, 100
Axial force/kN	3, 4, 5, 6
Pin length/mm	5.7
Tool shoulder diameter, <i>D</i> /mm	18
Pin diameter, <i>d</i> /mm	6
<i>D</i> / <i>d</i> ratio of tool	3.0
Tool pin geometry	Thread
Tool material	High carbon steel

Tensile specimens (as shown in Fig. 2) were machined in the traverse direction from the welded joints. Tensile test was carried out in a 100 kN servo controlled universal testing machine (Make: FIE-Bluestar, India; Model: UNITEK-94100). Microstructural analysis was carried out using an optical microscope (OM, Make: MEIJI, Japan; Model: MIL-7100) incorporated with an image analyzing software (Metal Vision MVLx1.0) and a scanning electron microscope (SEM, JEOL, Japan; Model: 6410LV) with an energy dispersive spectroscopy (EDS) analyzer. The specimens for metallographic examination were sectioned to the required sizes from the joint comprising weld zone (WZ), thermo mechanically affected zone (TMAZ), heat affected zone (HAZ) and base metal (BM) regions. Usual metallographic procedures were followed to polish the specimen and 5% hydrofluoric acid was used as an etchant to reveal the microstructure.

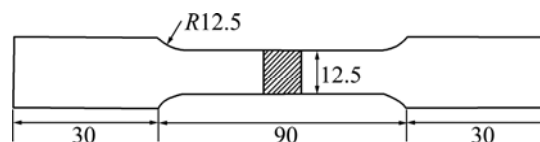


Fig. 2 Dimensions of tensile specimen (unit: mm)

3 Results

3.1 Tensile strength

Transverse tensile strengths of FSW joints are presented in Figs. 3–5. Three specimens were tested at each condition and average of the results of three specimens is presented in these figures. From these figures, it could be inferred that the tool rotation speed, welding speed and axial force have significant influence on tensile strength of the FSW joints of A356 aluminium alloy. Among four joints, the joint fabricated with a tool rotation speed of 1000 r/min showed a higher tensile

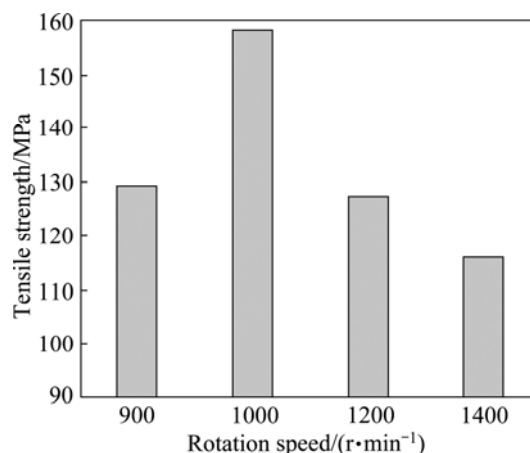


Fig. 3 Effect of rotational speed on tensile strength (Welding speed 75 mm/min; Axial force 5 kN)

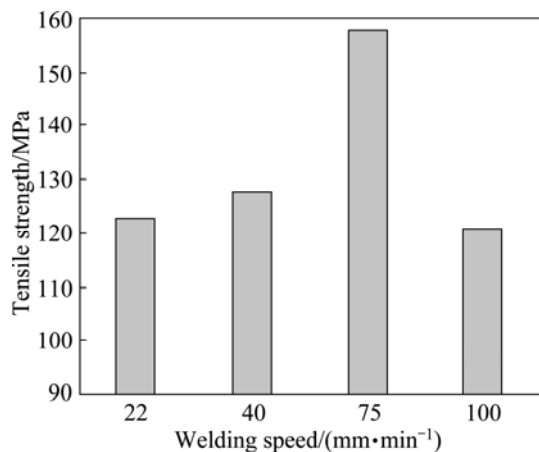


Fig. 4 Effect of welding speed on tensile strength (Rotational speed 1000 r/min; Axial force 5 kN)

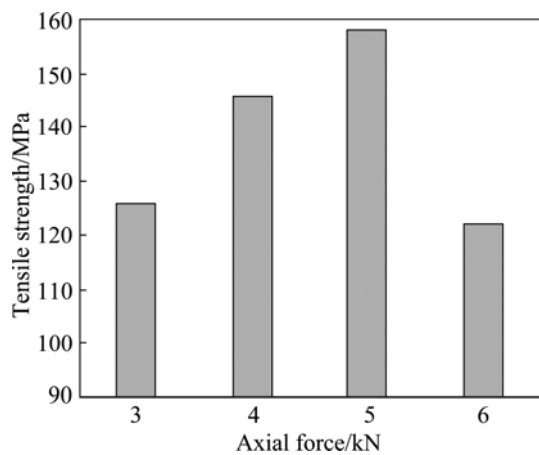


Fig. 5 Effect of axial force on tensile strength (Rotation speed 1000 r/min; Welding speed 75 mm/min)

strength compared to the other joints (Fig. 3). Similarly, the joint fabricated with a welding speed of 75 mm/min (Fig. 4) and the joint fabricated with an axial force of 5 kN (Fig. 5) exhibited superior tensile strength compared to their counter parts. In all the specimens, the failure location was found to be the weld region and hence a detailed macrostructure and microstructure analysis and hardness survey were carried out in the weld region.

3.2 Macrostructure

During FSW, the materials flow around the tool pin due to the heat generated by the friction and stirring action. FSW joints are prone to defects like pin hole, tunnel, cavity, kissing bond, cracks etc due to insufficient and excess heat input in the stir zone [10]. All the joints fabricated were analyzed at low magnification with an optical microscope to reveal the quality of weld zone. The macrographs of the weld zone are presented in Tables 3–5. Among the four tool rotation speeds used to fabricate the joints, the rotation speed of 1000 r/min produced defect-free weld. Similarly, the joint fabricated using a welding speed of 75 mm/min contained no defect. An axial force of 5 kN also yielded defect-free joint. The presence of the defects could be one of the reasons for reduction in tensile strength compared to defect-free welds.

3.3 Microhardness and microstructure

The measured values of microhardness in the weld region are presented in graphical forms shown in Figs. 6–8. The microstructure of the base metal consists of primary $\alpha(\text{Al})$ dendrites and interdendritic irregular Al–Si eutectic regions, namely, the distribution of Si

Table 3 Effect of tool rotation speed on macrostructure





Tool rotation speed/ (r·min ⁻¹)	Macrostructure		Name of defect and quality of weld	Probable reason
	RS	AS		
900			Crack at the middle of retreating side	Insufficient heat generation
1000			No defect	Sufficient heat generation
1200			Pin hole at the middle of the weld cross section in the retreating side	Excess turbulence of the plasticized metal
1400			Tunnel at the middle of the weld cross section in the retreating side	Abnormal stirring of the plasticized metal

Table 4 Effect of welding speed on macrostructure









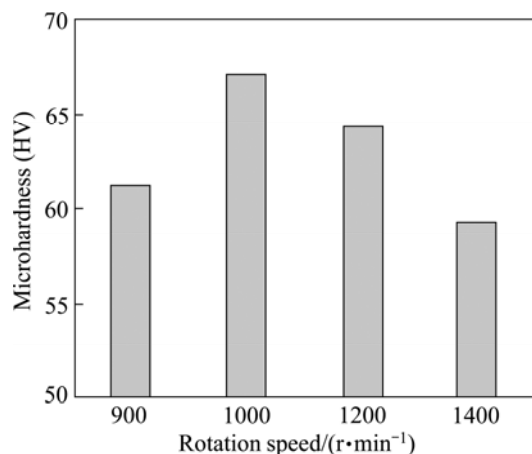
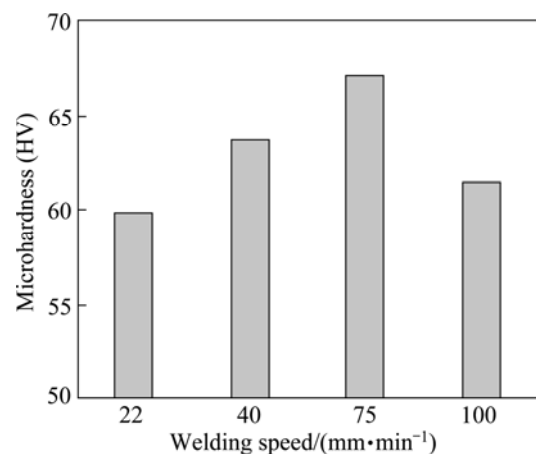
Welding speed/(mm·min ⁻¹)	Macrostructure		Name of defect and quality of weld	Probable reason
	RS	AS		
22			Tunnel at the top of the weld cross section in the retreating side	Excess turbulence of the plasticized metal
40			Tunnel at the middle of the retreating side	Excess turbulence of the plasticized metal
75			No defect	Sufficient heat generation
100			Piping defect at the retreating side	Insufficient heat generation

Table 5 Effect of axial force on macrostructure

Axial force/kN	Macrostructure		Name of defect	Probable reason
	RS	AS		
3			Tunnel at the middle of the retreating side	Insufficient heat due to the low axial force
4			Pin hole at the bottom of the retreating side	Insufficient flow of metal due to the low axial force
5			No defect	Sufficient flow of the plasticized metal
6			Tunnel at the retreating side and also thinning of metal	Thinning of metal due to the high axial force

RS–Retreating side; AS –Advancing side

**Fig. 6** Effect of rotation speed on microhardness (Welding speed 75 mm/min; Axial force 5 kN)**Fig. 7** Effect of welding speed on microhardness (Rotation speed 1000 r/min; Axial force 5 kN)

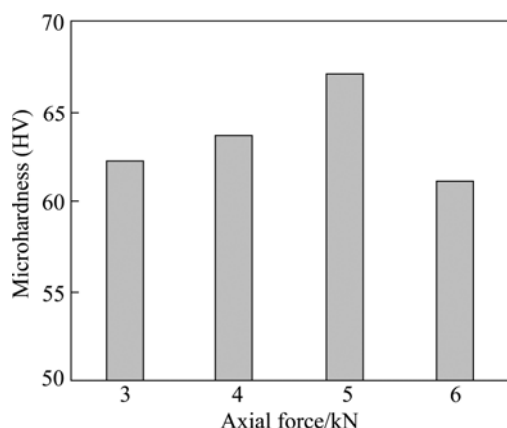


Fig. 8 Effect of axial force on microhardness (Rotation speed 1000 r/min; Welding speed 75 mm/min)

particles is not uniform throughout the aluminum matrix. Figures 9–11 show micrographs of the welded regions of all the joints observed under optical and scanning electron microscopes. There is significant breakup of Si particles and aluminium dendrite, and subsequently a uniform distribution of smaller Si particles is created in the $\alpha(\text{Al})$ matrix. It is due to the stirring action under plastic condition of the metal during FSW. This phenomenon was reported by other investigators also [11,12].

4 Discussion

4.1 Effect of tool rotation speed

In FSW, tool rotation speed results in stirring and mixing of material around the rotating pin which in turn increases the temperature of the metal. It appears to be the most significant process variable since it tends to influence the translational velocity. It is known that the maximum temperature observed to be a strong function of rotation speed. When the rotation speed increases, the heat input within the stirred zone also increases due to the higher friction heat which in turn result in more intense stirring and mixing of materials [13]. For the given welding speed and axial force, the increase of rotation speed beyond 1000 r/min produces tunnel defect in the retreating side due to the abnormal stirring. The turbulence of softened metal is not consolidated in the retreating side (Table 3). Similar phenomenon was reported by KIM et al [14] for the rotation speed greater than 700 r/min on ADC12 aluminium alloy. The tensile strength of the joint made with 1000 r/min is higher because of the sound joint with optimum heat input in the stir zone, where the strength is reduced with the increase of the rotation speed due to the formation of defects. The higher tensile strength is also attributed to the uniform distribution of fine eutectic Si particles in the aluminium matrix of the stir zone (Fig. 9(f)) whereas the

reduction of the strength is due to the coarse eutectic Si particles and non homogeneous distribution in the matrix [15]. This is due to the turbulence of softened metal at higher rotation speeds in which the broken Si particles are clustered to be coarse and segregated ones (Figs. 9(g) and (h)).

4.2 Effect of welding speed

The translation of tool moves the stirred material from the front to the back of the pin. The rate of heating of thermal cycle during FSW is a strong function of the welding speed [16]. During FSW thermal cycle, most of the Mg_2Si precipitates, the primary strengthening phases in A356, dissolved into the aluminium matrix. Fast cooling of FSW thermal cycle retains these solute atoms [17]. LIM et al [18] investigated the tensile behaviour of AA6061 aluminum alloy and opined that the main cause of the change in the tensile behaviour of friction stir welded AA 6061-T651 alloy with varying welding condition was the amount of plastic flow per unit time rather than the heat generated during the solid welding. They also observed severe clustering of coarse Mg_2Si precipitates in the tensile fractured area under each welding condition and the clustering was more significant in the specimens joined at low welding speeds.

Among the four joints fabricated using different welding speeds, the joints fabricated using a welding speed of 75 mm/min exhibited a higher tensile strength due to the formation of fine eutectic Si particles uniformly distributed in the aluminium matrix and also the absence of defects in the stir zone (Fig. 10(g)). The joints fabricated at welding speed of 22 mm/min consist of coarser Si particles and banded structure in the stir zone (Fig. 10(e)) which in turn reduces the joint strength. Similarly, the joints fabricated at welding speed of 40 mm/min consist of channel defect at the retreating side of the stir zone and coarser Si particles (Fig. 10(f)). The optimum heat input and the distribution of fine Si particles are the reasons for the enhancement of joint strength at welding speed 75 mm/min under constant rotation speed of 1000 r/min.

4.3 Effect of axial force

Material flow in the weld zone is influenced by the extrusion process, where the applied axial force and the motion of the tool pin propel the material after it has undergone the plastic deformation. The shoulder force is directly responsible for the plunge depth of the tool pin into the work piece and load characteristics associated with linear friction stir welding [19]. As the axial load increases, both hydrostatic pressure beneath the shoulder and the temperature in the stir zone will increase. It is

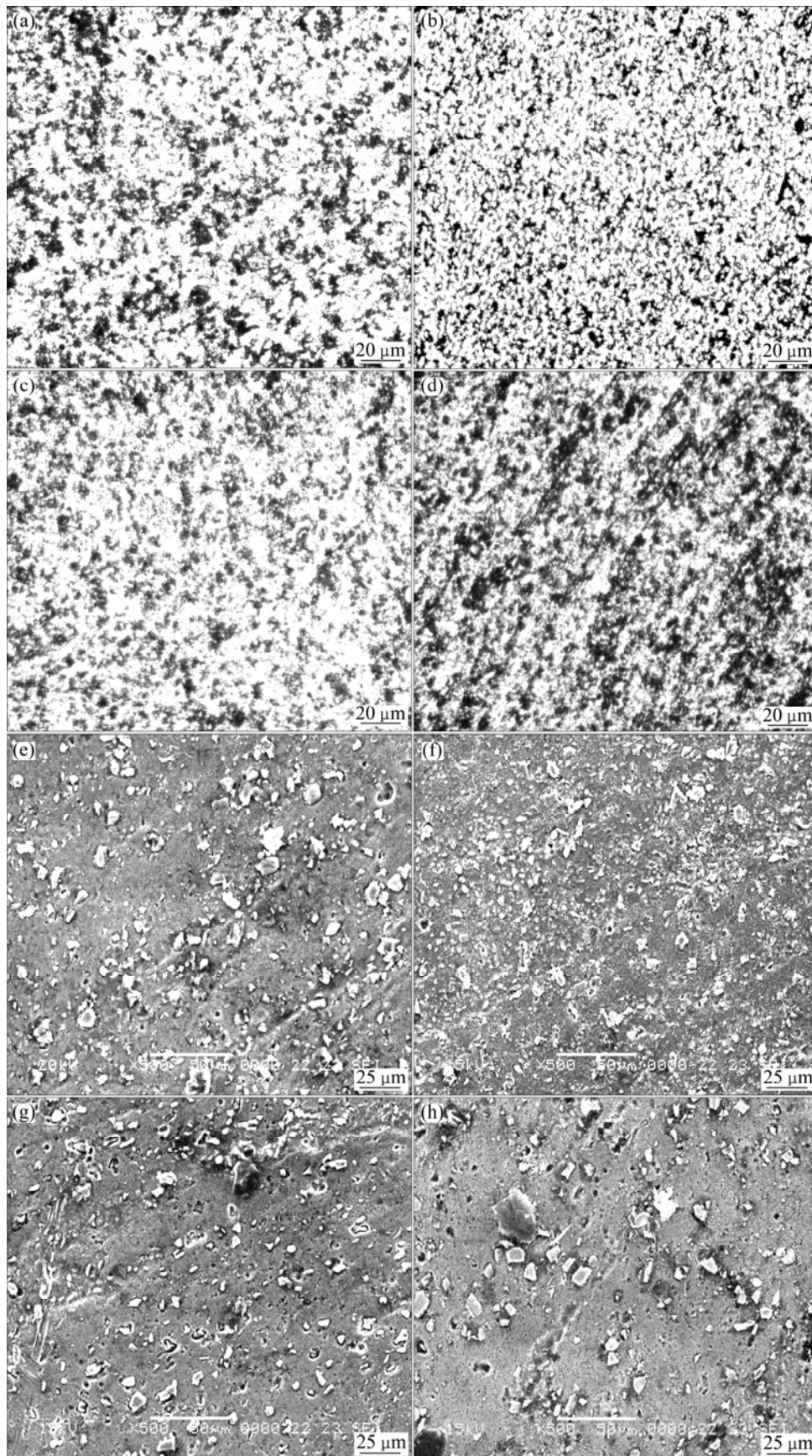


Fig. 9 Optical (a, b, c, d) and SEM (e, f, g, h) images showing effect of rotation speed on microstructure of welded region (Welding speed 75 mm/min; Axial force 5 kN): (a), (e) 900 r/min; (b), (f) 1000 r/min; (c), (g) 1200 r/min; (d), (h) 1400 r/min

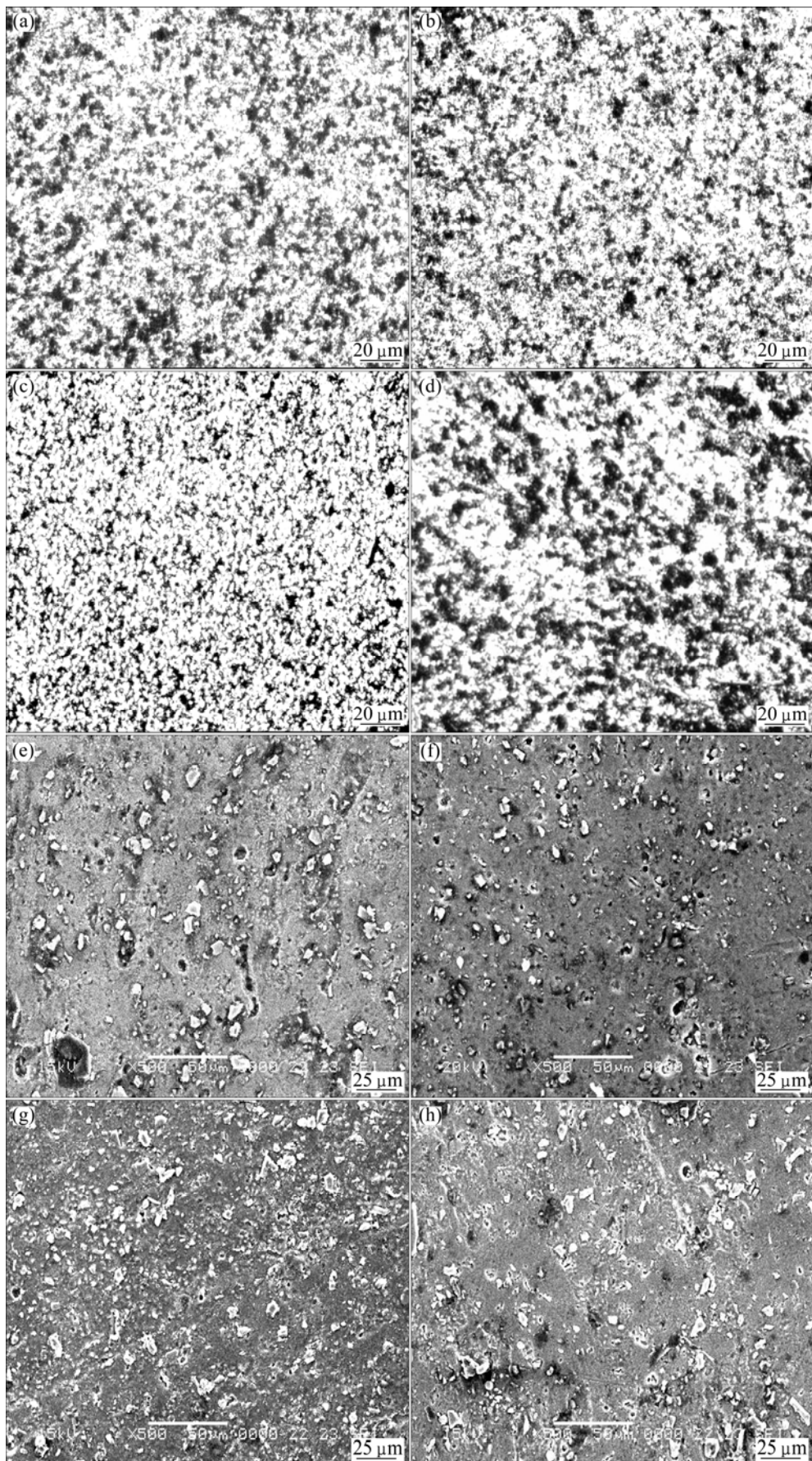


Fig. 10 Optical (a, b, c, d) and SEM (e, f, g, h) images showing effect of welding speed on microstructure of welded region (Rotation speed 1000 r/min; Axial force 5 kN): (a), (e) 22 mm/min; (d), (f) 40 mm/min; (c), (g) 75 mm/min; (d), (h) 100 mm/min

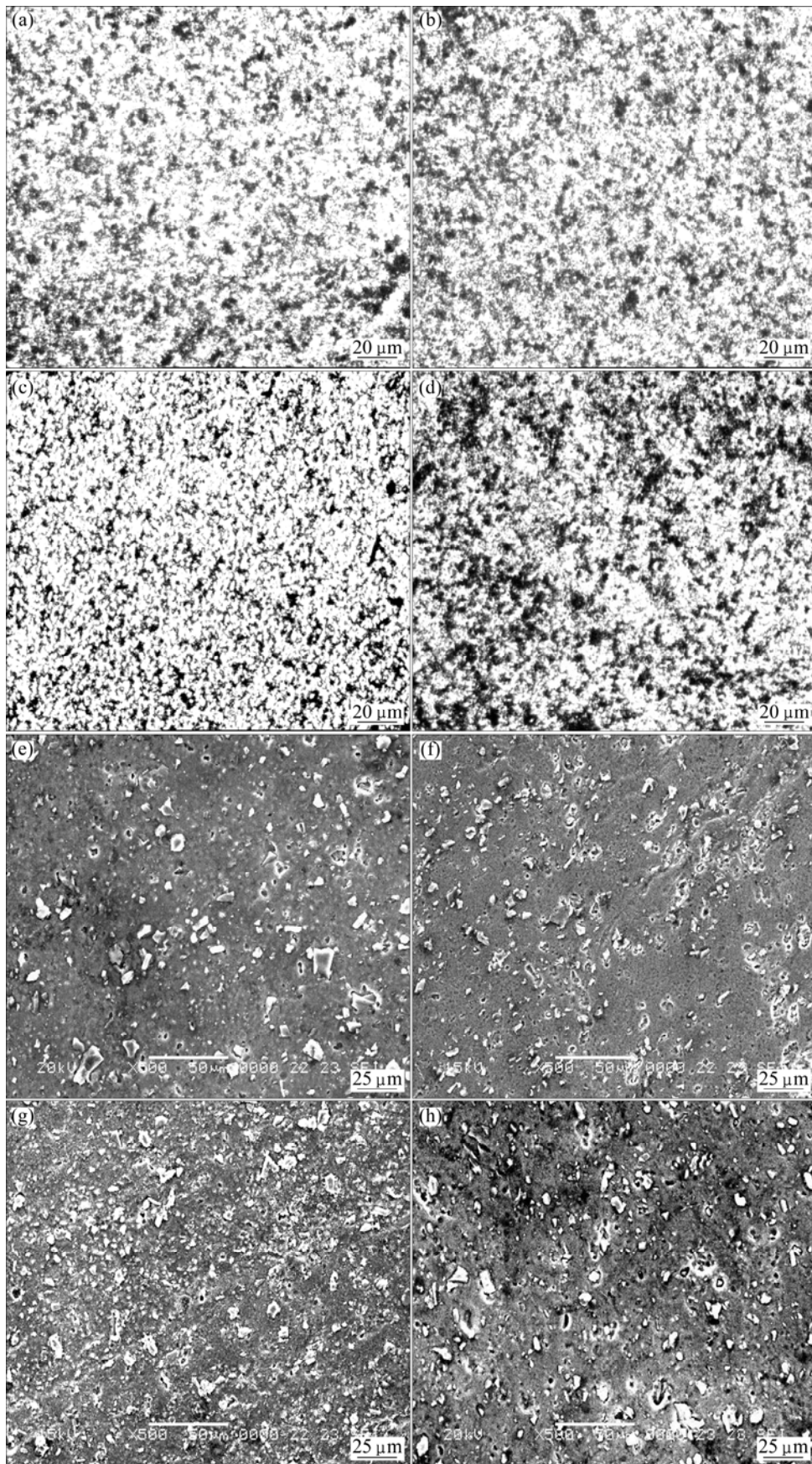


Fig. 11 Optical (a, b, c, d) and SEM (e, f, g, h) images showing effect of axial force on microstructure of weld region (Rotation speed 1000 r/min; Welding speed 75 mm/min): (a), (e) 3 kN; (b), (f) 4 kN; (c), (g) 5 kN; (d), (h) 6 kN

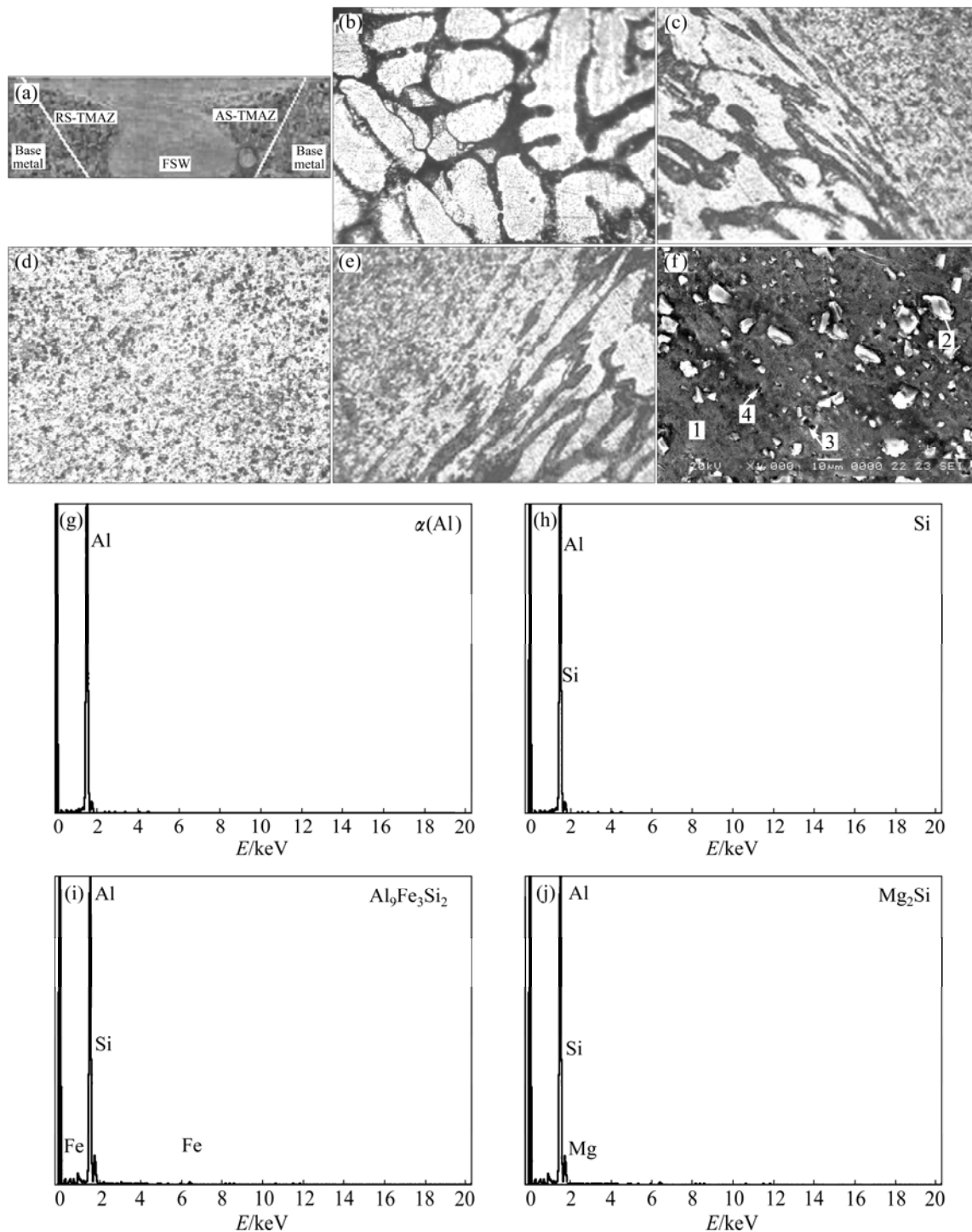


Fig. 12 Micrographs and EDS results under optimized conditions: (a) Macrograph; (b) OM image of base metal; (c) OM image of RS-TMAZ; (d) OM image of FSW; (e) AS-TMAZ; (f) SEM image; (g) Location 1; (h) Location 2; (i) Location 3; (j) Location 4

well known that the lower axial load results in defect in the weld because of insufficient coalescence of transferred material [20]. OUYANG et al [21] reported that at steady state, the shoulder force varies depending upon the rotation speed. An increase in the rotation speed results in drop in the initial axial force with increasing time. The difference in the measured forces is due to the decrease of the material flow stress at elevated weld

temperature. KRISHNAN [22] studied the mechanism of onion ring formation in the friction stir welds of aluminium alloys and found that the degree of material mixing and inter-diffusion, the thickness of deformed aluminium lamellae and material flow patterns highly depend upon the geometry of the tool, welding temperature, and material flow stress in turn depends on the axial force. Hence, the axial force must be optimized

to get FSP zone with good consolidation of metal and without thinning of the base material [23].

Of the four axial force levels used to fabricate the joints, the joint fabricated with an axial force of 2 kN resulted in pin hole defect at the top of the retreating side due to the insufficient material flow and the microstructure consisted of coarse eutectic Si particles (Fig. 11(e)), even though uniform distribution in the aluminium matrix. Similarly, the joint fabricated with 3 kN axial force exhibited the same pattern but the microstructure consisted of slightly finer Si particles than the joint made with 2 kN (Fig. 11(f)). But the joint fabricated with 5 kN axial force consisted of fine, eutectic Si particles with uniform distribution throughout the aluminium matrix (Fig. 11(g)) due to the sufficient flow of softened material. This may be the reason for higher tensile strength of the joints fabricated with 5 kN axial force compared to their counterparts.

From the experimental results of macrostructure, microstructure, micro hardness and joint strength, it is found that the joint fabricated using rotation speed 1000 r/min, welding speed 75 mm/min and axial force 5 kN exhibited superior tensile strength compared to other joints. This particular joint was analyzed in detail by optical microscopy (OM), scanning electron microscopy (SEM) and electron dispersive spectrum (EDS) and the results are presented in Fig. 12. The SEM image shows the distribution of eutectic Si particles and EDS results reveal the composition of the matrix and particles.

5 Conclusions

1) Among the twelve joints fabricated, the joint fabricated using the process parameters of tool rotation speed 1000 r/min, welding speed 75 mm/min and axial force 5 kN yielded a higher tensile strength compared to other joints.

2) Defect-free weld region, higher hardness of weld region and very fine, uniformly distributed eutectic Si particles in the weld region are found to be the important factors attributed for the higher tensile strength of the above joints.

Acknowledgement

The authors are grateful to the Department of Manufacturing Engineering, Annamalai University, Annamalaiagar, Tamil Nadu, India for extending the facilities of Metal Joining Laboratory and Materials Testing Laboratory to carryout this investigation.

References

[1] SHTRIKMAN M M. Current state and development of friction stir welding part 3 [J]. *Welding International*, 2008, 22(11): 806–815.

[2] SHARMA S R, MA Z Y, MISHRA R S. Effect of friction stir processing on fatigue behavior of A356 alloy [J]. *Scripta Materialia*, 2004, 51(3): 237–241.

[3] MA Z Y, MISHRA R S, MAHONEY M W. Superplasticity in cast A356 induced via friction stir processing [J]. *Scripta Materialia*, 2004, 50(7): 931–935.

[4] LIM S G, KIM S, LEE C G, KIM S J. Tensile behavior of friction-stir-welded A356-T6/Al 6061-T651Bi-alloy plate [J]. *Metallurgical and Materials Transactions A*, 2004, 35(9): 2837–2843.

[5] SANTELLA M L, ENGSTROM T, STORJOHANN D, PAN T Y. Effects of friction stir processing on mechanical properties of the cast aluminum alloys A319 and A356 [J]. *Scripta Materialia*, 2005, 53(2): 201–206.

[6] NAKATA K, KIM Y G, FUJII H, TSUMURA T, KOMAZAKI T. Improvement of mechanical properties of aluminum die casting alloy by multi-pass friction stir processing [J]. *Materials Science and Engineering A*, 2006, 437(2): 274–280.

[7] MA Z Y, SHARMA S R, MISHRA R S. Effect of friction stir processing on the microstructure of cast A356 aluminum [J]. *Materials Science and Engineering A*, 2006, 433(1–2): 269–278.

[8] KIM Y G, FUJII H T, TSUMURA T, KOMAZAKI T, NAKATA K. Effect of welding parameters on microstructure in the stir zone of FSW joints of aluminum die casting alloy [J]. *Materials Letters*, 2006, 60(29–30): 3830–3837.

[9] BALASUBRAMANIAN V. Relationship between base metal properties and friction stir welding process parameters [J]. *Materials Science and Engineering A*, 2008, 480(1–2): 397–403.

[10] CHEN Hua-bin, YAN Keng, LIN Tao, CHEN Shan-ben, JIANG Cheng-yu, ZHAO Yong. The investigation of typical welding defects for 5456 aluminum alloy friction stir welds [J]. *Materials Science and Engineering A*, 2006, 433(1–2): 64–69.

[11] MA Z Y, SHARMA S R, MISHRA R S, MAHONEY M W. Microstructural modification of cast aluminum alloys via friction stir processing [J]. *Materials Science Forum*, 2003, 426–432: 2891–2896.

[12] SHARMA S R, MA Z Y, MISHRA R S. Effect of friction stir processing on fatigue behavior of A356 alloy [J]. *Scripta Materialia*, 2004, 51(3): 237–241.

[13] MISHRA R S, MA Z Y. Friction stir welding and processing [J]. *Materials Science and Engineering R*, 2005, 50: 1–78.

[14] KIM Y G, FUJII H, TSUMURA T, KOMAZAKI T, NAKATA K. Three defect types in friction stir welding of aluminum die casting alloy [J]. *Materials Science and Engineering A*, 2006, 415(1–2): 250–254.

[15] MA Z Y, SHARMA S R, MISHRA R S. Microstructural modification of as-cast Al–Si–Mg alloy by friction stir processing [J]. *Metallurgical and Materials Transactions A*, 2006, 37(12): 3323–3336.

[16] LEE W B, YEON Y M, JUNG S B. The improvement of mechanical properties of friction-stir-welded A356 Al alloy [J]. *Materials Science and Engineering A*, 2003, 355(1–2): 154–159.

[17] MA Z Y, SHARMA S R, MISHRA R S. Effect of multiple-pass friction stir processing on microstructure and tensile properties of a cast aluminum–silicon alloy [J]. *Scripta Materialia*, 2006, 54(9): 1623–1626.

[18] LIM S G, KIM S, LEE C G, KIM S J. Tensile behaviour of friction stir welded Al 6061-T651 [J]. *Metallurgical and Materials Transactions A*, 2004, 35(9): 2829–2835.

[19] KIM Y G, FUJII H, TSUMURA T, KOMAZAKI T, NAKATA K. Effect of welding parameters on microstructure in the stir zone of FSW joints of aluminum die casting alloy [J]. *Materials Letters*, 2006, 60(29–30): 3830–3837.

- [20] KUMAR K, SATISH V KAILAS. On the role of axial load and the effect of interface position on the tensile strength of a friction stir welded aluminium alloy [J]. *Materials and Design*, 2008, 29(4): 791–797.
- [21] OUYANG J H, KOVACEVIC R. Material flow during friction stir welding (FSW) of the same and dissimilar aluminum alloys [J]. *Journal of Material Engineering and Performance*, 2002, 11(1): 51–63.
- [22] KRISHNAN K N. On the formation of onion rings in friction stir welds [J]. *Materials Science and Engineering A*, 2002, 327(2): 246–251.
- [23] REN S R, MA Z Y, CHEN L Q. Effect of welding parameters on tensile properties and fracture behavior of friction stir welded Al–Mg–Si alloy [J]. *Scripta Materialia*, 2007, 56(1): 69–72.

搅拌摩擦焊工艺参数对铸态 A356 铝合金抗拉强度的影响

M. JAYARAMAN¹, V. BALASUBRAMANIAN²

1. Paavaai Group of Institutions-Integrated Campus, School of Engineering, NH-7, Paavaai Vidhya Nagar, R. Puliyampatti, Puduchatram (Post) Namakkal – 637 018, Tamil Nadu, India;
2. Centre for Materials Joining & Research (CEMAJOR), Department of Manufacturing Engineering, Annamalai University, Annamalai Nagar–608 002, Tamil Nadu, India

摘 要: A356 是一种高强度铝硅铸造态合金, 广泛用于食品、化工、船舶、电器和汽车行业。熔焊这种铸造合金时存在许多问题, 如孔隙、微裂隙、热裂等。然而, 用搅拌摩擦焊(FSW)来焊接这种铸造态合金可以避免上述缺陷发生。研究了搅拌摩擦焊工艺参数对铸造态 A356 铝合金抗拉强度的影响; 对旋转速度、焊接速度和轴向力等工艺参数进行优化; 从宏观和微观组织分析角度对焊接区的质量进行分析; 对焊接接头的抗拉强度进行了测定, 并对抗拉强度与焊缝区硬度和显微组织的相关性进行了研究。在旋转速度 1000 r/min、焊接速度 75 mm/min 和轴向力 5 kN 的条件下得到的焊接接头具有最高的抗拉强度。

关键词: A356 铝合金; 摩擦搅拌焊; 工具旋转速度; 焊接速度; 轴向力; 抗拉强度

(Edited by Hua YANG)